Journal of Applied Polymer Science

Networked Cellulose Entrapped and Reinforced PEO-Based Solid Polymer Electrolyte for Moderate Temperature Applications

Yarjan Abdul Samad, Ali Asghar, Boor Singh Lalia, Raed Hashaikeh
Materials Science and Engineering Program, Masdar Institute of Science and Technology, Abu Dhabi 54224, UAE
Correspondence to: R. Hashaikeh (E-mail: rhashaikeh@masdar.ac.ae)

ABSTRACT: A novel solid polymer electrolyte (SPE) composed of poly (ethylene oxide) (PEO) and networked cellulose (NC) is developed for moderate temperature applications typically 50 to 100°C. The SPE thus formed demonstrates enhanced strength; high thermal and appropriate electrochemical stability. NC is a high strength polymeric material with a network structure possessing open spaces in its construction. The NC open spaces shrink on drying. The SPEs are formed by solution casting different amounts of NC in dissolved PEO. NC was formed by the acid hydrolysis and regeneration of microcrystalline cellulose (MCC). SEM, TEM and in-situ optical images revealed that the dissolved PEO solidified around the suspended NC and the open structure of NC entraps PEO upon drying. NC provides structural and thermal stability to the SPE. With an addition of 15wt% NC in SPE there was about five-time increase in both tensile as well as storage modulus measured via tensile testing and Dynamic mechanical analysis (DMA) respectively. The enhancement of mechanical strength is explained using the Zener model. Cyclic voltammetry (CV) and linear sweep voltammetry (LSV) studies validated that the electrochemical stability window of PEO+15 wt %NC with salt and that of neat PEO with salt are analogous. © 2013 Wiley Periodicals, Inc. J. Appl. Polym. Sci. 129: 2998–3006, 2013

KEYWORDS: cellulose and other wood products; batteries and fuel cells; mechanical properties; membranes; microscopy

Received 18 June 2012; accepted 15 January 2013; published online 15 February 2013
DOI: 10.1002/app.39033

INTRODUCTION

Conventionally, liquid and gel electrolytes have been used in electrochemical devices such as lithium ion batteries. These electrolytes are not stable at high temperatures and often leak, jeopardizing the long-term stability of such device.[1,2] Furthermore, the growth of lithium dendrites is promoted in such low modulus electrolytes which lead to the short circuit of a lithium battery and eventually to the heating up and melting of the lithium metal. Alternatively, solid polymer electrolytes (SPE) have been developed which aim to alleviate this problem.[3–5] SPEs are of great importance in lithium batteries as they eliminate the need for extensive sealing.

So far, the most extensively studied host polymer for the electrolyte in lithium batteries is the readily available poly (ethylene oxide) (PEO). PEO is a semicrystalline polymeric material which is used in applications ranging from pharmaceutical drugs to paper production and most recently in water retention.[6–8] PEO complexed with Li salt is a good ionic conductor at temperatures near 100°C. However, it has poor mechanical properties which may result in creep of the electrolyte and allow the electrodes to come into contact and short circuit the cell. There have been several attempts to modify PEO with different organic and inorganic fillers, cross-linked networks and block or comb branch polymerization to make the PEO mechanically and thermally stable with enhanced electrochemical performance.[7–13] Thus, current problems with PEO-based solid polymer electrolytes, when used at high temperatures, are cyclability and safety. This is mainly due to the reactivity of the lithium metal anode and the degradation in mechanical strength of PEO. There have been attempts to resolve the former problem by modification of the electrolyte so that a favorable passivation on Lithium is formed assuring efficient lithium deposition-stripping processes.[14] Solution to the latter problem can be twofold: (1) an enhancement of the ionic conductivity at low temperatures, and (2) enhancement of the mechanical properties at higher temperatures without significant loss in the ionic conductivity.

Each year, plant, algae, and some bacteria produce billions of tonnes of organic matter half of which is made up of biopolymer cellulose, this makes cellulose the most abundant organic molecule on the planet.[15] Cellulose is the main component of wood, cotton, cell-wall of most plants and other textile fibers such as linen, hemp, and jute. In the plant cell wall, cellulose is the reinforcing constituent of high strength and modulus due to

© 2013 Wiley Periodicals, Inc.

its extended chain structure.[16] So, the cellulosic cell wall in the plants provides structural integrity by encapsulating the cell components inside. Cellulosic constituents are gaining increasing importance due to their high strength and stiffness and high potential as a reinforcing agent.[17–19] Cellulose has been used to prepare separators for lithium ion batteries.[20] In addition, cellulose nanowhiskers have already been used as reinforcement for polymer electrolytes.[9,10]

In this work we have used the network of cellulose chains in order to encapsulate as well as reinforce PEO to synergistically provide mechanical stability to the SPE at high temperatures without compromising its electrochemical properties indispensable for use in a Lithium battery. Networked cellulose (NC) suspension in water is synthesized by opening the structure of microcrystalline cellulose by acidic hydrolysis using sulphuric acid. Appropriate amounts of NC and PEO are used to fabricate the SPEs. Structural, thermal, thermo-mechanical and electrochemical properties of fabricated SPEs are studied and a mechanism of the structure evolution is proposed.

EXPERIMENTAL

Materials

Microcrystalline Cellulose (MCC) (M_W = 350,000) was provided by FMC Biopolymer (Philadelphia, PA). Sulfuric acid (99.9%), Polyethylene Oxide (M_W = 4000, 000), Ethanol and Lithium perchlorate ($LiClO_4$) were purchased from Aldrich (St. Louis, MO).

Preparation of NC Suspension

Acid Hydrolysis of MCC was performed using a Varian®dissolution system following a procedure reported earlier by our group.[21] The dissolution system bath is adjusted to 5°C temperature using ice cubes. Sulfuric acid of 70% (w/w) concentration is added to a vessel and is stabilized to reach 5°C. Subsequently, 10 g MCC is added to 100 mL sulfuric acid and the resulting solution is mixed for 30 min at 5°C at 250 rpm to form a viscous and transparent liquid of cellulose completely dissolved in sulfuric acid. Ethanol which is kept at 5°C is added to the dissolved cellulose solution to regenerate the cellulose. The mixture is further mixed for 10 min to allow for complete regeneration of cellulose. The resulting material is centrifuged at 4700 rpm and 4°C temperature and the acidic top layer is decanted. The centrifugation process is repeated three times to remove sulfuric acid. The centrifugation process resulted in separating the precipitated material from the spent liquor. The precipitate was collected again and dialyzed (against running tap water) for 3 days until the pH of the suspension reached 6–7. The NC suspension was completely homogenized using a mechanical homogenizer (IKA-T25 ULTRA-TURRAX) and heated at 50°C for 5 h at an agitation of 250 rpm to yield a thick suspension with a concentration of 4.5% (w/w) in water.

Fabrication of SPEs

PEO solution in water and NC are mixed at room temperature and 20 wt % of $LiClO_4$ is dissolved in the mixture with respect to the total weight of the PEO and NC. Different amounts of NC are mixed with PEO as shown in Table I. The amount of $LiClO_4$ is fixed for all the samples. The different compositions of PEO, NC, and $LiClO_4$ are solution casted in Teflon boats to obtain polymeric electrolyte films. They are left to dry in the ambient conditions for a week and were kept in a vacuum of 100 kPa for 24 h at 80°C in order to remove all the moisture content and directly transferred to an Argon filled glove box (MBraun, Germany) having moisture and oxygen contents < 0.1 ppm.

Table I. Variation of Mechanical Behavior with the Composition of SPEs

PEO (wt %)	NC (wt %)	$LiClO_4$ (wt %)	Tensile modulus (MPa)
100	0	20	N/A
99	1	20	N/A
98	2	20	3.8
95	5	20	8.4
90	10	20	17.3
85	15	20	19.2
80	20	20	20
75	25	20	43
70	30	20	53
65	35	20	54.2
60	40	20	108
50	50	20	N/A
60	60	20	N/A

N/A, sample is not able to handle for tensile testing; N/A* = film could not be formed.

Characterization for Mechanical Integrity

Tensile Testing. Young's modulus and tensile strength of the PEO/$LiClO_4$ and PEO+xwt%NC/ $LiClO_4$ solid SPEs were measured by Instron (Model No. 5982) equipped with load cell of 5 kN at strain rate of 0.5 mm/min. The dog-bone shaped specimens having length 65 mm cut from the solid electrolyte of thickness ~150–200 μm. Three samples for each composition were tested to ensure the reproducibility of the test results.

Dynamic Mechanical Analysis. PerkinElmer DMA 8000 was used to investigate the variation of storage modulus, from 30°C until the rupture, in tension deformation mode at the frequency of 1 Hz and heating rate 2°C/min. Rectangular samples of dimensions 10 mm × 3.3 mm were used with thicknesses ranging ~150–200 μm.

Thermal Analysis. Thermal stability of the SPEs was characterized by DSC (PerkinElmer DSC 4000) and TGA (PerkinElmer TGA 4000) analysis. DSC was performed at heating rate of 10°C/min over temperature range of 25–445°C under nitrogen atmosphere. Thermo gravimetric analysis (TGA) of the composite SPE was studied in 25–800°C temperature range under nitrogen atmosphere with the scan rate of 10°C/min.

Electrochemical Analysis

Ionic conductivities of the SPEs were measured using Autolab-302N potentiostat/galvanostat in 1 MHz to 10 MHz frequency range. Blocking Stainless Steel electrodes were used to sandwich the SPEs for conductivity measurement. PEO/$LiClO_4$ and PEO

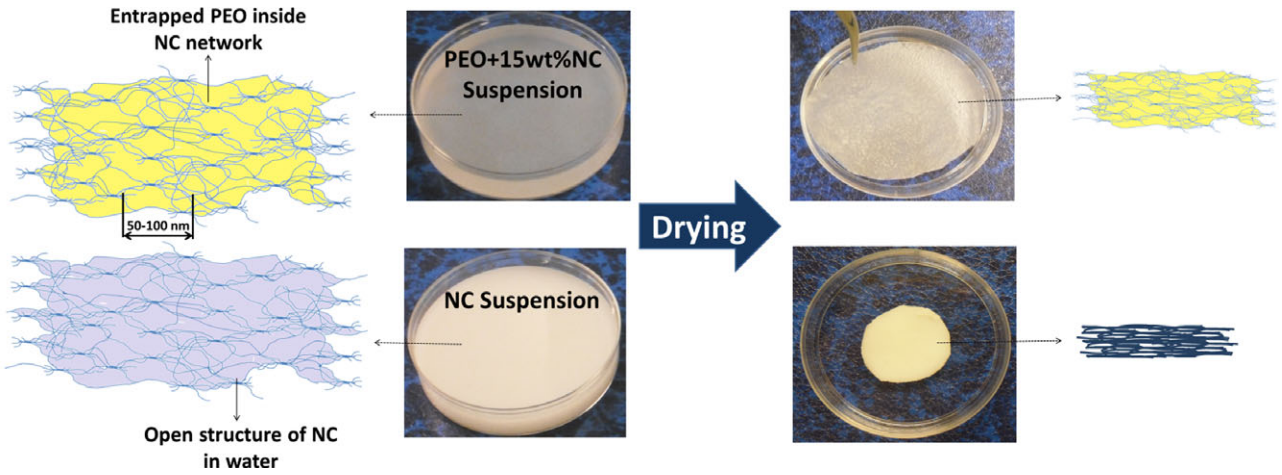

Figure 1. Schematic representation of the formation mechanism of SPEs from dissolved PEO and NC suspension. [Color figure can be viewed in the online issue, which is available at wileyonlinelibrary.com.]

+15 wt % NC/$LiClO_4$ were chosen for Linear Sweep voltammetry (LSV) and cyclic voltammetry (CV). LSV was sweep from 2.0 to 5.5 V (vs. Li^+/Li) at a scan rate of 1 mV/s while CV was done from 2.5 to 4.2 V at a scan rate of 0.1 mV/s. Both LSV and CV measurements were done at 80°C. For LSV, Li metal electrode was used as the counter electrode and reference and Stainless steel electrode (area = 0.25 cm^2) was used as the working electrode. Whereas $LiFePO_4$ (MTI corporation, USA) as working electrode and lithium foil as counter electrode and reference were used for CV measurement.

Structural and Morphological Analysis

Oven dried samples of NC and NC+PEO with and without $LiClO_4$ were loaded on a silicon substrate and X-ray diffractograms were obtained using an X-ray diffractometer (PANalytical, Emperean) operated at 45 kV and 40 mA with Ni-filtered Cu K_α (λ = 1.5056 Å) radiations in 5–70° theta range. A diffractogram of the silicon substrate is obtained and used to correct the diffractograms of the samples measured.

The sample for TEM was prepared using Focused ion beam (FIB) lamella lift out and thinning method. First, a layer of Chromium was deposited on the surface of the sample to get a SEM image of the sample while doing FIB milling. Then a protection layer of silicon and then platinum was made to protect the structure of the NC while milling with ion beam.

A lamella of 3*20*3 μm was lift out using a microprobe and was then thinned down to a thickness of only 150 nm which is sufficient for polymer materials to give atomic resolution in TEM. TEM images were taken by JEOL 2011 High Contrast Digital Transmission Electron Microscope. The images attached are bright field images produced by using a low intensity beam to minimize artifacts induced by the beam.

Networked cellulose 4.0 wt % suspensions was freeze dried and was used for scanning electron microscopy (SEM) in order to view the structure without any shrinkage that would occur in normal air drying. Freeze dried samples were dispersed on a conducting carbon tape and were then sputtered with a 4 nanometer thick Au-Pd layer in order to deposit an electron conducting layer to avoid charging effects while imaging. Solutions of PEO and PEO+NC were grown *in-situ* on a carbon tape to observe the growth under SEM. Samples were imaged in high vacuum in the FEI Quanta FEG 250. *In-situ* Optical microscopy of two PEO+NC samples were done at 50× by observing the growth of PEO+NC solution on glass slide.

RESULTS AND DISCUSSION

Structural and Morphological Analysis

The schematic in Figure 1 elaborates the formation of SPEs from the suspension of PEO+xwt%NC. When NC suspension is dried, it shrinks and forms a compact structure. Therefore, when NC gel is added to PEO, the open structure of NC accommodates part of dissolved PEO. Simultaneously, upon drying, PEO forms hydrogen bonds with NC and starts solidifying inside the NC network as described in Figure 1. Consequently, the SPE has entrapped PEO inside the NC network structure. Figure 2 shows that a neat PEO film melts after heating at 100°C for 30 min whereas the developed composite of PEO with 15 wt % NC is free standing after heating and shows complete dimensional stability.

Figure 3(a,b) shows optical images of the *in-situ* growth of PEO+5wt%NC and Figure 3(c,d) shows that of PEO+20wt%NC. It is clear that the PEO spherulites start growing from the suspended NC particles because they act as nucleation sites for dissolved PEO to solidify. Increasing NC content means increasing sites of nucleation for PEO to solidify resulting in smaller PEO spherulites as shown in the *in-situ* optical images.

TEM images of NC and SEM images of freeze dried NC gel sample, Figure 4(a,b), show a networked structure confirming the open structure of NC in suspension. In order to understand the growth of PEO spherulites, *in situ* growth of PEO was observed in SEM. Figure 4(c) shows *in situ* SEM image of the growth of PEO spherulites on carbon where carbon is acting as a nucleation site for dissolved PEO to solidify. PEO grows in similar fashion when NC is added and NC as shown in Figure 4(d) where it can clearly be seen that the PEO fibers are coming

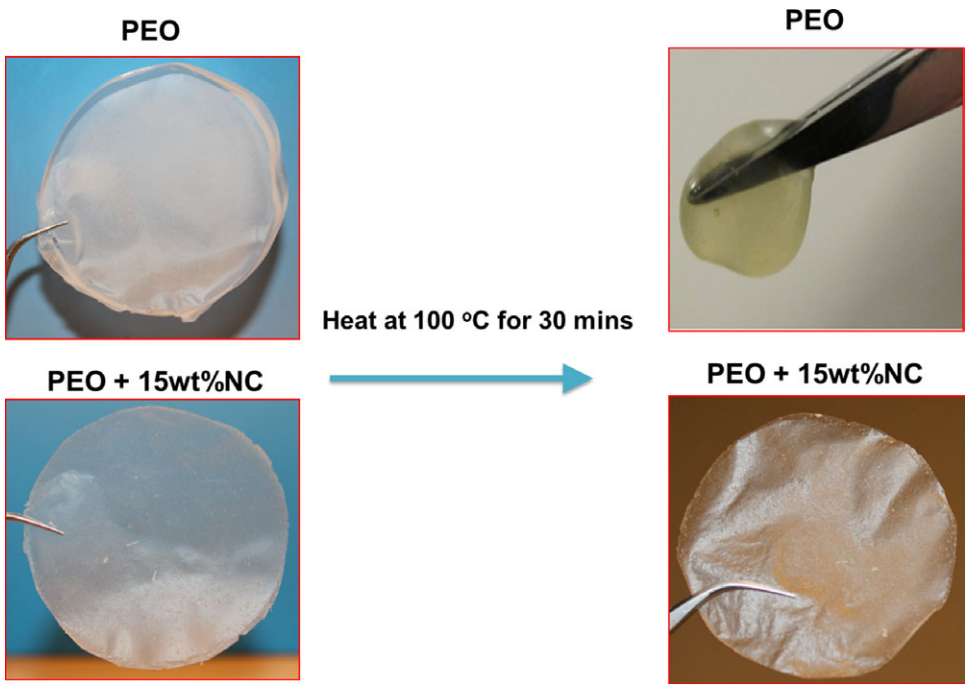

Figure 2. Description of PEO and NC interaction while drying (a) and demonstrating effect of temperature on PEO and PEO +15wt%NC. [Color figure can be viewed in the online issue, which is available at wileyonlinelibrary.com.]

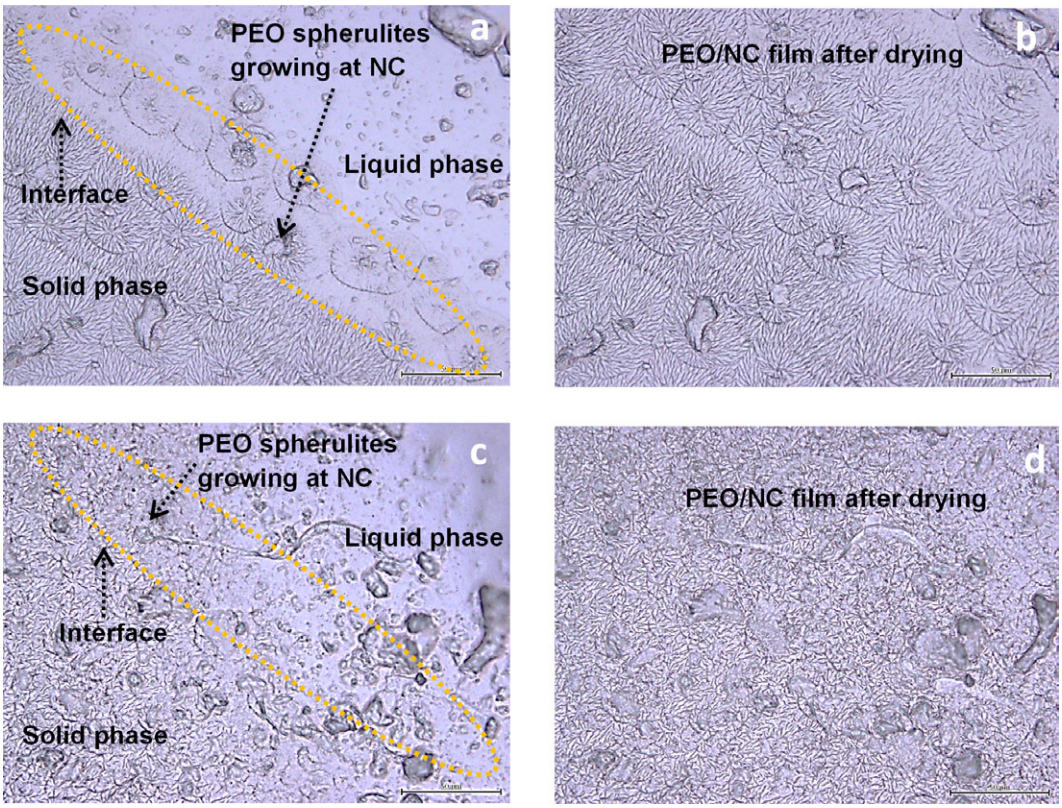

Figure 3. Optical images showing the in situ growth of PEO+5wt%NC before (a) and after (b) complete solidification and PEO+20wt%NC before (c) and after (d) complete solidification. The scale bar shown in the images is 50 μm. [Color figure can be viewed in the online issue, which is available at wileyonlinelibrary.com.]

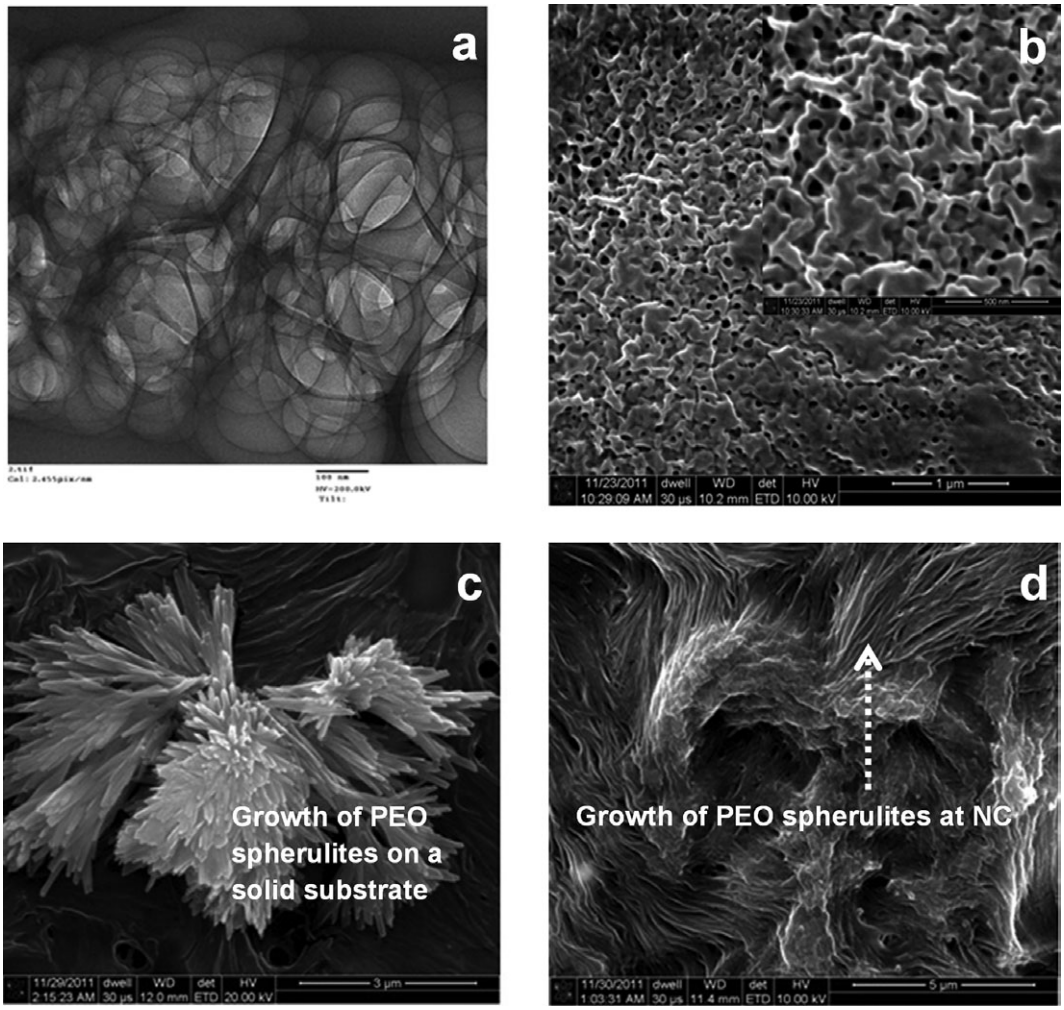

Figure 4. Micrographs of TEM with a scale of 100 nm (a) and SEM with a scale of 1 μm (b) of freeze dried NC. In-situ SEM images of PEO spherulites with a scale of 3 μm (c) and surface SEM image of PEO+15 wt%NC membrane with scale of 5 μm (d).

out of the NC particles confirming the initiation of their growth from NC.

XRD results of the samples without adding the $LiClO_4$ salt show a crystalline structure and the crystallinity is not altered significantly with increasing NC content as shown in Figure 5(a). XRD results of PEO+xwt%NC without salt are consistent with works reported elsewhere.[22] This can be explained because of the fact that the NC can reduce the spherulites sizes of PEO however on molecular level the order remains unchanged where alternate crystalline and amorphous regions exist in the material. XRD data of the samples with salt [Figure 5(b)] show a broad hump for all NC concentrations showing an amorphous structure. These results are in agreement with the DSC results showing no melting peak for PEO at 65°C.

Mechanical Integrity

The tensile tests of PEO/$LiClO_4$ and PEO+xwt% NC/$LiClO_4$ SPEs were carried out at ambient temperature. The tensile results are tabulated in Table I and indicate a significant increase in the tensile modulus of the SPEs with an increase in the NC content. It is believed that at molecular level there is hydrogen bonding between the cellulose network and EO groups, whereas, on a macroscopic scale, NC particles act as reinforcement to PEO. Since both PEO and NC are hydrophilic in nature, good interfacial properties are expected. The growth of the PEO spherulites initiate from the NC particles as shown in optical (In-situ) and SEM images in Figures 3(b) and 4(d) respectively. Thus the plastic deformation of PEO spherulites is restricted by the NC and the degree of restriction of deformation increases with increasing NC content. Similar results have been reported by reinforcing PEO with cellulose whiskers.[9]

The DMA results of the SPE without salt are shown in Figure 6. The DMA analysis of the SPEs is done at a frequency of 1Hz and 2°C/min heating rate from ambient temperature to the temperature at which they fail or their storage modulus values fall down below the limit of the equipment. At room temperature the amorphous regions of semi-crystalline PEO are already above their glass transition temperature. Therefore, DMA shows a rubbery behavior from 25°C to 60°C where the storage modulus is decreasing constantly with increasing temperature.

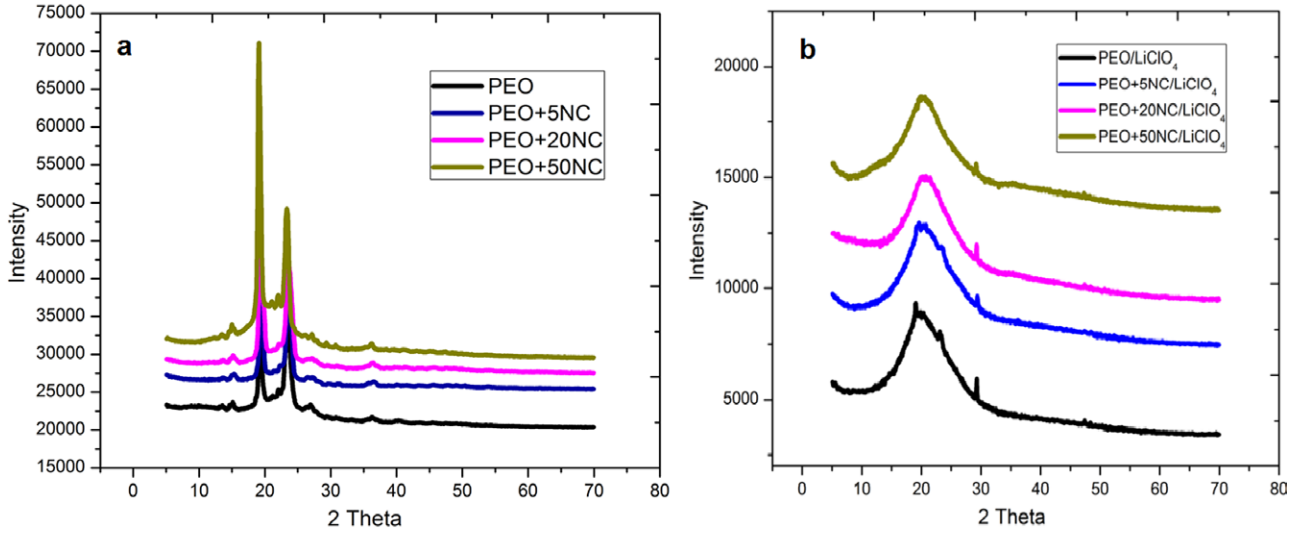

Figure 5. XRD of PEO+xwt%NC (a) and PEO+xwt%NC/$LiClO_4$ (b). [Color figure can be viewed in the online issue, which is available at wileyonlinelibrary.com.]

Above 60°C the crystalline regions of PEO melt and thus it has a viscous behavior and the storage modulus for pure PEO falls below the limits of the equipment. The storage modulus, which can be related to young's modulus; increases with increasing NC content at all temperatures due to high thermal stability of the NC phase in the SPEs and the enhanced interfacial properties between PEO and NC. Hence, DMA results are well in agreement with the tensile tests.

These results can be explained by the inductance and resistance i.e. the spring and the dashpot model of Zener.[23] In this model dashpot is the characteristic of viscous behavior whereas the spring represents the elastic behavior. At temperatures above 60°C PEO behaves like a viscous material indicated by a dashpot whereas PEO+15wt%NC is still a solid and can be shown with a spring and dashpot in parallel as shown in Figure 8(b). Below 60°C both PEO and PEO+15wt%NC possess viscous and elastic behavior in parallel, however, due to the melting of the crystalline parts of PEO at 60°C it behaves like a viscous material. PEO with NC has the viscous and elastic behavior in both the regions but the elastic behavior is more dominant below 60°C than after it, due to the presence of both crystalline PEO and NC at this temperature. Above 60°C the only elastic part in PEO+15wt%NC is due to the presence of NC. Hence the strain, at this temperature region, in PEO+15wt%NC will be determined as the ratio of stress vs the modulus and the stain in pristine PEO will be determined as the product of time with the ratio of stress vs viscosity of PEO.

Thermal Properties Analysis

Neat NC and PEO+xwt%NC/$LiClO_4$ samples were tested in DSC and TGA for their thermal behavior. The DSC results of the SPE show that there is no melting peak of the crystalline phase of PEO as shown in Figure 7(a). This is in agreement with previous studies showing that with the addition of 15–20 wt% $LiClO_4$ in polymer, PEO/$LiClO_4$ complexes suppress the melting peak at 65°C.[24,25] PEO with 20wt% $LiClO_4$ starts decomposing at around 340°C whereas the exothermic peak at 250°C indicates the decomposition of pure NC as shown in the DSC thermogram. Decomposition of pure NC is not as prominent as that of the SPE samples with salt because the salt is much more exothermic in nature than NC. The decomposition of all the SPE samples with different concentrations of NC falls between 250 and 340°C. Note that there is also a broad peak which is not very prominent at around 340°C corresponding to the decomposition of PEO inside the SPE which becomes less prominent with increasing NC content in SPE. TGA data, in Figure 7(b), of the PEO+xwt%NC, neat NC and neat PEO/$LiClO_4$ correspond very well with the DSC results showing that the weight loss for NC starts at 240°C and that of PEO/$LiClO_4$ starts at about 340°C. The decomposition of the samples with NC falls between 250 and 340°C temperatures. TGA also shows that there is a slight shift in the weight loss at 340°C which then disappears with increasing NC content showing

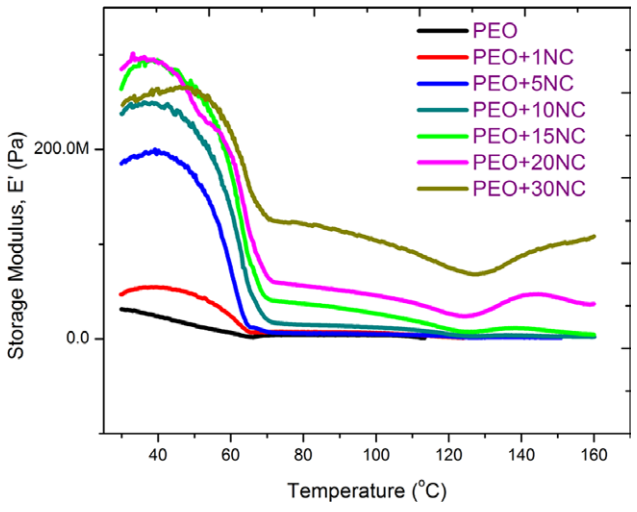

Figure 6. DMA results of PEO+xwt%NC without $LiClO_4$. [Color figure can be viewed in the online issue, which is available at wileyonlinelibrary.com.]

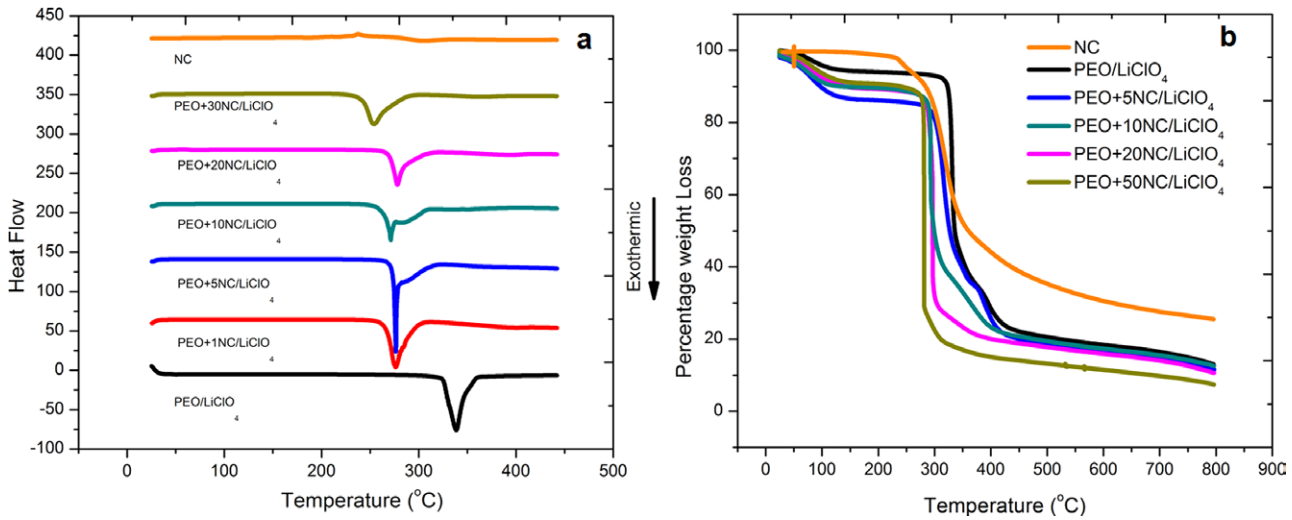

Figure 7. DSC (a) and TGA (b) results of PEO+xwt%NC/$LiClO_4$. [Color figure can be viewed in the online issue, which is available at wileyonlinelibrary.com.]

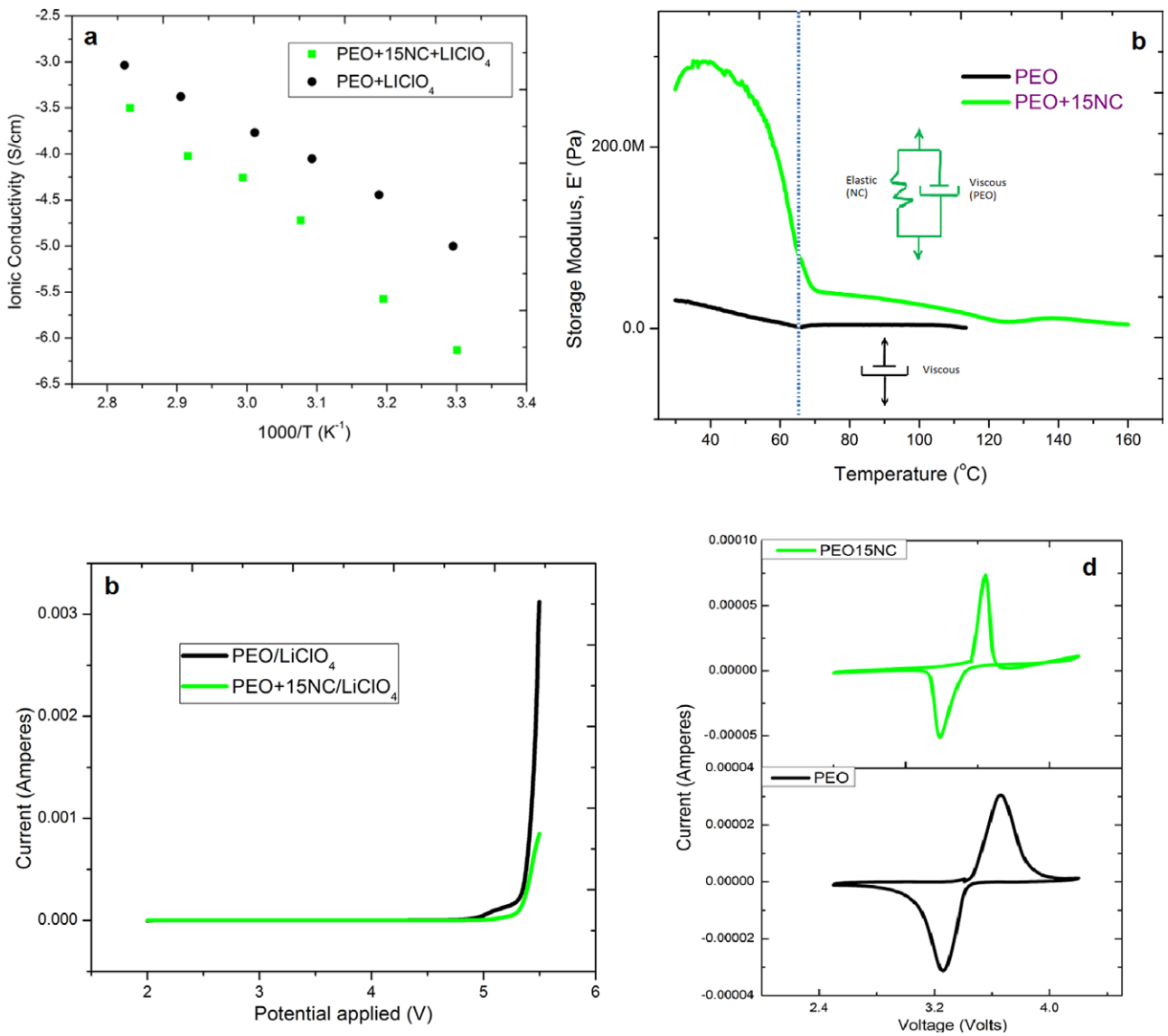

Figure 8. Arrhenius plot for PEO/$LiClO_4$ and PEO+15wt%NC/$LiClO_4$ (a) linear sweep voltammetry (b) and cyclic voltammetry of $LiFePO_4$/ (PEO/$LiClO_4$)/Li cell (c) and $LiFePO_4$/(PEO + NC/ $LiClO_4$)Li cell (d). [Color figure can be viewed in the online issue, which is available at wileyonlinelibrary.com.]

consistency with the DSC results. More importantly, TGA and DSC results show that the electrolyte samples are highly stable in temperatures up to 200°C and can thus be used for high temperature lithium metal batteries.

Electrochemical Analysis

Ionic conductivity of all the SPE samples were measured via impedance spectroscopy analysis after oven drying for 12 h at 50°C and keeping them in vacuum at 100 kPa for 24 h. Figure 8(a) shows the Arrhenius plot of conductivity of PEO/$LiClO_4$ and PEO+15NC/$LiClO_4$ vs. temperature. PEO/$LiClO_4$ displays highest conductivity of about 5×10^{-6} S/cm and 9×10^{-4} S/cm at 30 and 80°C respectively. PEO+15NC/$LiClO_4$ displays ionic conductivities of about 8×10^{-7} S/cm and 2.5×10^{-4} S/cm at 30 and 80°C respectively. The reduction in conductivity with the addition of 15 wt % NC is not significant at higher temperatures whereas the thermomechanical behavior of PEO+15NC is much superior to pristine PEO at all temperatures. As shown in the schematic in Figure 1, the entrapped PEO inside NC network acts as channels of ionic conduction whereas NC provides structural and thermal stability to the SPE at high temperatures. Commonly accepted explanation of ionic conductivity in PEO is assigned to the segmental motion of the amorphous regions.[26,27] It is believed that the stiff NC phase restricts segmental motions in PEO which is responsible for decreasing ionic conductivity with the addition of NC. These results match with the model developed by Sergiy Kalnaus and coworkers showing the reduction of conductivity with mechanical properties enhancement with the addition of non-conducting filler phase.[28] As part of an extension to this work, the effective conductivity and effective mechanical strength of our SPEs can be measured using this model after taking the electrode materials into consideration. Nonetheless high strength and modulus of the SPEs allows the use of high amounts of plasticizers such as organic solvents and Ionic liquids in order to increase the ionic conductivity to an acceptable range without greatly jeopardizing the mechanical integrity of the polymer. This effect becomes more prominent at NC contents higher than 15wt%. Therefore, PEO+15wt%NC/ $LiClO_4$ was chosen for LSV and CV studies. Linear Sweep voltammograms, Figure 8(b), shows the stability of the SPEs up to 5 V potential (vs. Li^+/Li) and decomposition of the SPEs starts at around 5 V. Generally Lithium ion batteries' cell potential can reach a voltage of 4.5 V during charging. Thus the SPEs, described in this work, possess electrochemical stability required for lithium secondary batteries. The anodic electrochemical stability of PEO+15wt%NC/ $LiClO_4$ is rather slightly higher than that of neat PEO/ $LiClO_4$. CV of the Li/$LiFePO_4$ cell using PEO/$LiClO_4$ and PEO+15wt%NC/$LiClO_4$ were performed to check the reversible intercalation-deintercalation of Li^+ ions on the SPE/$LiFePO_4$ and stripping-destripping of Li^+ ion on the Li/SPE interfaces in 2.5 to 4.2 V potential ranges. The voltammograms are shown in Figure 8(c,d), redox peaks reveal a reversible reaction at the $LiFePO_4$/SPE interface.

CONCLUSIONS

This study illustrates the synthesis and characterization of PEO and NC to be applied as SPEs for Li and Li ion batteries. In the wet NC gel, cellulose exists in an open network structure. The drying behavior of the NC gel allows it to entrap PEO and provide structural integrity and stability up to 250°C. This stability was tested using several techniques such as: Tensile testing, DMA, TGA, DSC and *in-situ* observation. The developed SPEs have an enhanced stability over neat PEO up to 250°C. With an addition of 15 wt % NC in PEO there is more than an order of magnitude increase in the storage modulus at 70°C. The fabricated electrolyte samples have a reasonable ionic conductivity of the order of 10^{-5} S/cm for PEO/$LiClO_4$ and PEO+15wt%NC/$LiClO_4$, at 60°C. The fabricated SPE using this method has an anodic electrochemical stability of 5V (vs. Li^+/Li) that allows them to be used in lithium batteries.

REFERENCES

1. Sommeling, P. M. Chemistry **2004**, *137*.
2. Tarascon, J. M.; Armand, M. *Nature* **2001**, *414*, 359.
3. Geiculescu, O. E.; Yang, J.; Blau, H.; Bailey-Walsh, R.; Creager, S. E.; Pennington, W. T.; DesMarteau, D. D. *Solid State Ionics* **2002**, *148*, 173.
4. Agrawal, R.; Pandey, G. *J. Phys. D: Appl. Phys.* **2008**, *41*, 223001.
5. Izuchi, S.; Ochiai, S.; Takeuchi, K. *J. Power Sources* **1997**, *68*, 37.
6. Yu, X. Y.; Xiao, M.; Wang, S. J. *J. Appl. Polym. Sci.* **2010**, *115*, 2718.
7. Scrosati, B.; Croce, F.; Persi, L. *J. Electrochem. Soc.* **2000**, *147*, 1718.
8. Kumar, B.; Scanlon, L. G. *Solid State Ionics* **1999**, *124*, 239.
9. Azizi Samir, M. A. S.; Chazeau, L.; Alloin, F.; Cavaillé, J.-Y.; Dufresne, A.; Sanchez, J.-Y. *Electrochimica Acta* **2005**, *50*, 3897.
10. Azizi Samir, M. A. S.; Mateos, A. M.; Alloin, F.; Sanchez, J.-Y.; Dufresne, A. *Electrochimica Acta* **2004**, *49*, 4667.
11. Basak, P.; Manorama, S. V. *Solid State Ionics* **2004**, *167*, 113.
12. Yue, Z.; McEwen, I. J.; Cowie, J. M. G. *Solid State Ionics* **2003**, *156*, 155.
13. Higa, M.; Fujino, Y.; Koumoto, T.; Kitani, R.; Egashira, S. *Electrochim. Acta* **2005**, *50*, 3832.
14. Choi, Y. K.; Park, J. G.; Chung, K.; Choi, B. D.; Kim, W. S. *Microchem. J.* **2000**, *64*, 227.
15. Perez, S.; Samain, D. In Advances in Carbohydrate Chemistry and Biochemistry; Horton, D. (Ed.); **2010**, *64*, p 25.
16. Nishino, T.; Takano, K.; Nakamae, K. *J. Polym. Sci. Part B: Polym. Phys.* **1995**, *33*, 1647.
17. Tashiro, K.; Kobayashi, M. *Polymer* **1991**, *32*, 1516.
18. Svagan, A. J.; Azizi Samir, M. A. S.; Berglund, L. A. *Biomacromolecules* **2007**, *8*, 2556.
19. Bengtssona, M.; Baillifa; M. L.; Oksman, K. *Compos. Part A: Appl. Sci. Manufact.* **2007**, *38*, 1922.
20. Chiappone, A.; Naira, J. R.; Gerbaldi, C.; Jabbour, L.; Bongiovanni, R.; Zeno, E.; Beneventi, D.; Penazzi, N. *J. Power Sources* **2011**, *196*, 10280.

21. Hashaikeh, R.; Abushammala, H. *Carbohydr. Polym.* **2011**, *83*, 1088.

22. Linfeng, H.; Zilong, T.; Zhongtai, Z. *J Power Sources* **2007**, *166*, 226.

23. McCrum, N. G.; Buckley, C. P.; Bucknall, C. B. Principles of Polymer Engineering, OUP, **1997**, *139*.

24. Scrosati, B. *J. Electrochem. Soc.* **1990**, *136*, 2774.

25. Wieczorek, W.; Florjancyk, Z.; Stevens, J. R. *Electrochim. Acta*, **1995**, *40*, 2251.

26. Kumar, B.; Rodrigues, S. J.; Koka, S. *Electrochim. Acta* **2002**, *47*, 4125.

27. Fullerton-Shirey, S. K.; Maranas, J. K. *Macromolecules* **2009**, *42*, 2142.

28. Kalnaus, S.; Sabau, A. S.; Tenhaeff, W. E.; Dudney, N. J.; Daniel, C. *J. Power Sources* **2012**, *201*, 280.